Journal of Power Sources 196 (2011) 4811–4815

Contents lists available at ScienceDirect

Journal of Power Sources

journal homepage: www.elsevier.com/locate/jpowsour

Short communication

Nano-sized SiO_x/C composite anode for lithium ion batteries

Jing Wang[a], Hailei Zhao[a,b,*], Jianchao He[a], Chunmei Wang[a], Jie Wang[a]

[a] School of Materials Science and Engineering, University of Science and Technology Beijing, Beijing 100083, China
[b] Beijing Key Lab. of New Energy Materials and Technology, Beijing 100083, China

ARTICLE INFO

Article history:
Received 27 October 2010
Received in revised form 15 January 2011
Accepted 20 January 2011
Available online 26 January 2011

Keywords:
Silicon oxide
Carbon coating
Core–shell structure
Anode
Lithium ion battery

ABSTRACT

Nano-sized SiO_x/C composite with core–shell structure is prepared by a modified Stöber method. After heat-treatment, the O/Si ratio in SiO_x/C composite is near 1 and the core of SiO_x presents a structure composing of amorphous Si clusters and ordered SiO_2 domains. SiO_x/C composite anode shows high specific capacity (ca. 800 mAh g^{-1}), excellent cycling stability, good rate-capability but low initial coulombic efficiency. Li_2O and Li_4SiO_4 may generate in the initial lithiation process, which, combining with the carbon shell, can buffer the volume change caused by the alloying of Si with Li, and thereby improving the cycling stability of electrode. The nano feature of SiO_x/C particle and the electronic conductive nature of carbon coating layer ensure the good rate-capability of SiO_x/C electrode.

1. Introduction

With the growing demand for high capacity secondary batteries, the low capacity limit of graphite (372 mAh g^{-1}) has become a barrier in wider applications, thus high capacity alternatives, e.g. silicon (Si) and Si-based intermetallics/composite, have been received a particular attention for use in the next-generation lithium-ion batteries. The theoretical capacity of Si to form $Li_{22}Si_5$ is 4190 mAh g^{-1} [1] ensuring the electrodes with high specific capacity and high energy per unit volume. Meanwhile, the lithiation/delithiation voltage of Si is a few hundreds millivolts above lithium, resulting in the electrode with safe feature. However, the alloying/de-alloying of Li with Si causes a drastic volume change, leading to cracking or pulverizing of the electrode and thus rapid capacity decay [2]. Improvements are made by employing nano-sized particles [3], controlling crystallization [2,4], forming composite with other elements [5], and coating with carbon [1,6,7]. The cycling performance of Si-based anode materials, however, is still far from commercialization, and much effort is being put into the further improvement [8].

SiO-based materials attract much attention recent years because Li_2O, generated by the reaction of Li with SiO during the initial lithiation process, can act as a buffer component to improve the cycling performance of electrode [1,7,8]. Meanwhile, the resulted nano-sized Si, uniformly distributing in Li_2O matrix, renders the electrode with a high specific capacity. To improve the electronic conductivity and prevent the agglomeration of the derived nanoscale Si, SiO/C composites are usually prepared from SiO and graphite via high-energy ball-milling [9]. Reducing the particle size is an effective way to enhance the ionic conductivity by shortening the diffusion distance of lithium ions and to stabilize the geometric structure of Si-based electrode [9]. In this work, a carbon coated SiO_x nanocomposite (SiO_x/C) with a core–shell structure was prepared via a solution route. The structure and electrochemical characteristics of SiO_x/C nanocomposite as an anode material were characterized. The synthesized SiO_x/C nanocomposite exhibited a high specific capacity and a good cyclic performance.

2. Experimental

2.1. Preparation of SiO_x/C core–shell composite

The precursor solution of SiO_2 nanoparticles was prepared by a modified Stöber method with tetraethylorthosilicate (TEOS), absolute ethanol and ammonia as starting materials [10]. For the preparation of core–shell structured SiO_x/C nanocomposite, epoxy resin as carbon source was added into the SiO_2 microemulsion, followed by vigorous stirring at 100 °C until a gel was formed. The gel was placed in an alumina crucible with cover and then heated in a furnace at 650 °C for 0.5 h in air to get SiO_x/C powder. For structure comparison, commercially available SiO powder was used to elucidate the structural characteristic of the prepared SiO_x/C composite.

* Corresponding author at: School of Materials Science and Engineering, University of Science and Technology Beijing, Beijing 100083, China. Tel.: +86 10 82376837; fax: +86 10 82376837.
E-mail address: hlzhao@ustb.edu.cn (H. Zhao).

0378-7753/$ – see front matter © 2011 Elsevier B.V. All rights reserved.
doi:10.1016/j.jpowsour.2011.01.053

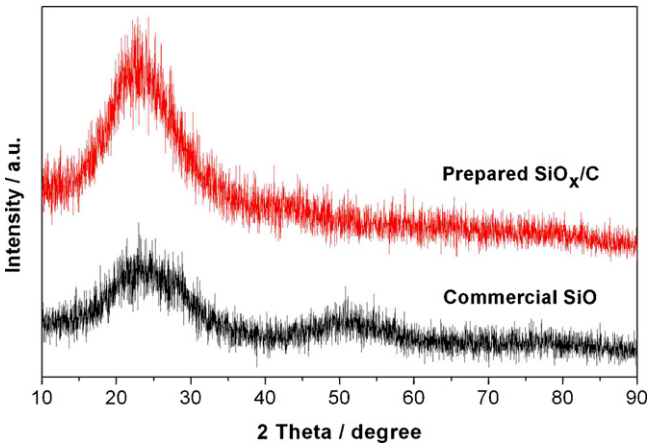

Fig. 1. XRD patterns of prepared SiO_x/C composite and commercial SiO.

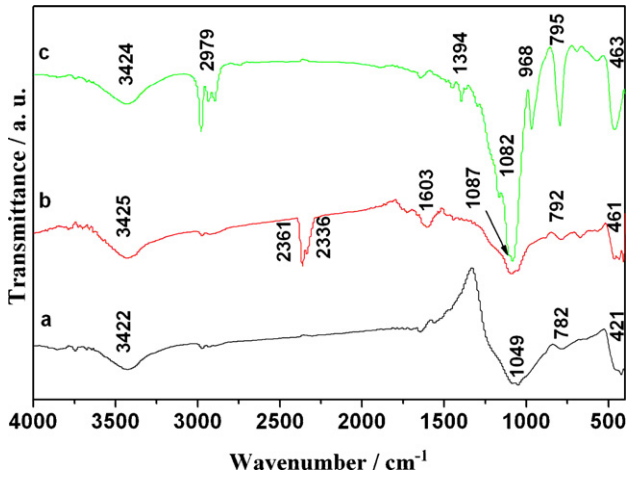

Fig. 2. FTIR spectra of the commercial SiO (a), the prepared SiO_x/C composite (b) and its precursor (c).

2.2. Physical characterization

Structural analysis was carried out by using a powder X-ray diffraction (XRD, Rigaku D/max-A X-ray diffractometer) with Cu Ka radiation. The particle morphology was characterized by an H-800 transmission electron microscope (TEM), a JEM-2010 high-resolution transmission electron microscope (HR-TEM), and a SUPRA55 field-emission scanning electron scanning electron microscope (FE-SEM). The lattice structure of the synthesized materials was analyzed by selected area electron diffraction (SAED). A Fourier transform infrared spectroscope (FTIR, Themo Nicolet 670FT-IR) was used for recording the FTIR spectra of the samples in the range 400–4000 cm^{-1}.

For the HR-TEM observation of the cycled electrodes, the model cells at different stages which were discharged to 0.01 V and charged to 3.0 V after three cycles, were dismantled in an Ar-filled glove box. The electrode materials were scraped from the Cu current collector and rinsed in anhydrous, dimethyl carbonate (DMC) to eliminate residual salts. The powders were dispersed ultrasonically in acetone, and then the samples were selected with a copper grid covered with carbon film. To avoid exposure to oxygen and water, the grid were rapidly transferred into the chambers.

2.3. Electrochemical characterization

Sample electrodes were prepared by coating slurries containing the active material powders (70 wt.%), acetylene black (15 wt.%), and polyvinylidene fluoride (15 wt.%) on copper foil. After drying at 120 °C in a vacuum oven for 24 h, the copper foil with electrode materials were then punched into circular discs with a diameter of 8 mm to use as the working electrode [11]. The mass load of the active material was about 2–3 mg cm^{-2} in all electrodes. Lithium foil was used as counter electrode. The electrolyte consisted of 1 M $LiPF_6$ in a non-aqueous solution of ethylene carbonate (EC), ethyl methyl carbonate (EMC) and dimethyl carbonate (DMC) with a volume ratio of 1:1:1. The cell was assembled in an Ar-filled glove box. Galvanostatic cycling test was carried out at different constant current densities between 0.01 and 3.0 V vs. Li/Li^+ with a Land CT2100 battery test system.

3. Results and discussion

The XRD pattern of SiO_x/C composite after calcination at 650 °C for 0.5 h is shown in Fig. 1, which is somewhat different from that of the commercial SiO [12]. A broad peak located in the 2θ range of 20–30° is assignable to SiO_2 with low crystallinity, and the peak around 43° is ascribed to carbon. No peak corresponding to Si is observed. The FTIR spectrum of the prepared SiO_x/C composite, accompanying with that of the precursor of SiO_x/C composite powder and the commercial SiO powders as comparison, is shown in Fig. 2. The broad absorption centered at ca. 3420 cm^{-1} is due to adsorbed water. Several weak peaks from 2860 to 2980 cm^{-1} are observed in precursor spectrum, which represent the C–H bonds of alkyl groups [13]. The absence of these peaks in calcined SiO_x/C composite spectrum indicates the decomposition of alkyl groups after calcination. The peaks nearby 1100 cm^{-1}, 790 cm^{-1} and 460 cm^{-1} are assigned to Si–O bond [13]. The different peak intensities for Si–O bond in the three samples demonstrate that the prepared SiO_x/C composite has similar Si–O structure with commercial SiO powder rather than its precursor. For the precursor, the small shoulder to the peak of 1100 cm^{-1} at 960 cm^{-1} implies the presence of asymmetric stretching vibration of Si–OH groups and the peak at 1394 cm^{-1} is due to the C–N bond. They disappear from SiO_x/C composite. Contrast with commercial SiO, SiO_x/C composite has twin peaks at 2361 and 2336 cm^{-1}, and peak around 1600 cm^{-1}. The former is assignable to CO_2, while the latter is due to C=C bond. During the calcination process, CO_2 was produced and adsorbed on the composites surface due to the carbonization of organic groups in precursor. SiO_x/C composite exhibits a similar FTIR spectrum with commercial SiO except for the peaks due to CO_2 and C=C bond, indicating that SiO_x/C composite has the same siloxane network as commercial SiO.

The FE-SEM image of SiO_x/C composite powders is shown in Fig. 3a. Many near-spherical particles with a size ca. 100 nm and a small amount of aggregated large particle are observed. EDS analysis reveals that the Si/O ratio in SiO_x/C composite is near 1. TEM image (Fig. 3b) indicates that SiO_x particles with a size of ca. 30 nm are coated with a carbon thin film (as indicated by the arrows), forming a core–shell structure. HR-TEM observation (Fig. 3c) demonstrates that SiO_x particle is actually composed of two distinct parts, well-ordered and disordered parts. In the ordered part, lattice fringe is observed, and the lattice spacing agrees with SiO_2 (2 1 0) plane spacing. The SAED image shows three circles, and the lattice plane spacing calculated from these circles is consistent well with SiO_2 (1 1 0), (2 1 0), and (4 0 0). It is reasonable to state that the ordered structure is SiO_2. Taking into account the fact that the Si/O atomic ratio in the composite is near 1 according to the EDS result, the nanocrystalline SiO_2 should be mixed with amorphous Si (disordered part). This result is consistent with the random-mixture

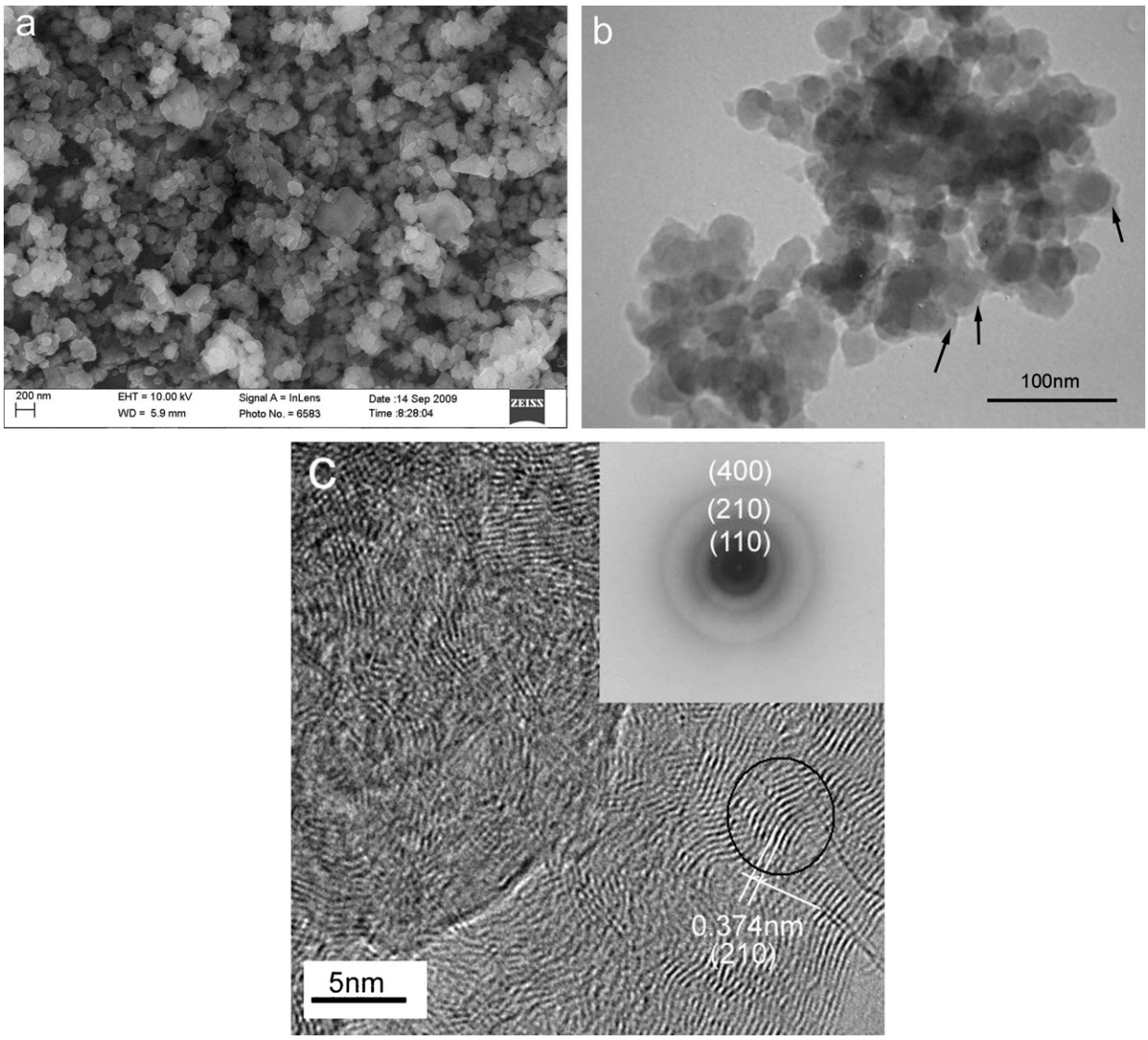

Fig. 3. (a) FE-SEM micrograph of SiO_x/C powders, (b) TEM micrograph of SiO_x/C powder and (c) HR-TEM micrograph of SiO_x/C particle (inset: electron-beam diffraction pattern of the ordered part).

model, where SiO is described as a mixture of cluster Si and SiO_2 [12,14].

The electrochemical performance of SiO_x/C composite electrode is plotted in Fig. 4. There is a distinct plateau at ca. 0.8 V in the first lithiation profile (Fig. 4a), which is ascribed to the decomposition of electrolyte and the formation of SEI film [2,5]. SiO_x/C electrode displays a random Li-ion insertion/extraction behavior without any Li–Si alloying plateau, most probably due to the poor crystallinity of Si component in the electrode, which is similar with the reported works [15,16]. SiO_x/C electrode shows a high initial capacity of 2223.6 mAh g^{-1} but a low initial coulombic efficiency of 47.3%. Nevertheless, it exhibits high reversible capacity, ca. 800 mAh g^{-1}, and excellent cycling stability (Fig. 4b). The high reversible capacity is attributed to the nano-scaled SiO_x particles. Although carbon was existing in the SiO_x/C composite (about 31.4 wt.% according to the chemical analysis), it should contribute less to the whole specific capacity of electrode due to its relatively low theoretical capacity. The nano-scaled SiO_2 domains in SiO_x particles may be active and can react with Li-ions to form Si and Li_4SiO_4 during initial lithiation process [17,18], as revealed by the following HR-TEM observation. The formed Li_2O and Li_4SiO_4 are inactive, thus can play a buffer role to accommodate the volume change on the subsequent cycling and prevent the electrochemical agglomeration of nano-sized Si clusters during lithiation/delithiation process, thereby making great contribution to the excellent cycling performance of SiO_x/C electrode. On the other hand, the carbon layer on the SiO_x particle surface can also make contribution to the volume change controlling of electrode during cycle. The SiO_x/C electrode maintains an excellent cycling stability at a high current density and exhibits good performance recoverability after switching back to a low current density (Fig. 4c). The nano-scale characteristics of SiO_x/C particles ensure the fast Li-ion transport in electrode, and the carbon coating layer provides the good electronic conductivity of the active material. Both of them guarantee the excellent rate-capability of SiO_x/C composite electrode.

To clarify the lithiation/delithiation mechanism, HR-TEM and electron-beam diffraction examination were performed on the SiO_x/C composite electrodes after discharging to 0.01 V and charging to 3.0 V. The results are shown in Fig. 5(a) and (b), respectively. Some ordered domains are observed in both of the lithiated and delithiated electrodes. There are two and three circles in the SAED patterns, as shown in the inset of Fig. 5(a) and (b), which agree well with Li_4SiO_4 ($\bar{2}$ 2 0) and (2 1 3) planes, and (1 3 0), ($\bar{2}$ 2 0) and (1 3 1) planes, respectively. Based on the SAED results, the ordered struc-

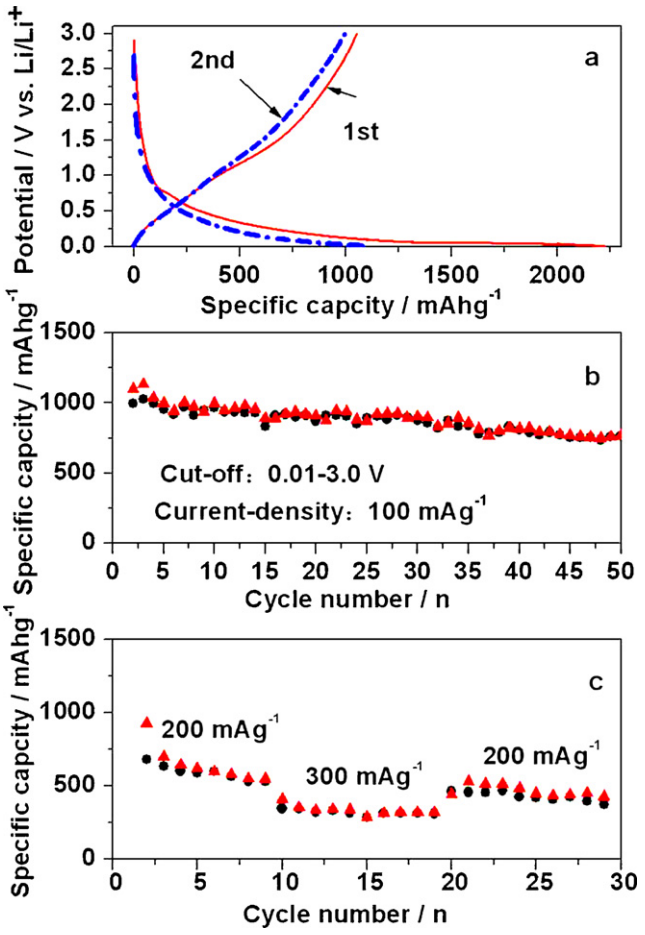

Fig. 4. Electrochemical performance of SiO_x/C composite: charge and discharge profiles for the first and second cycles (a), cycling performance from second cycle (b), and rate-capability (c).

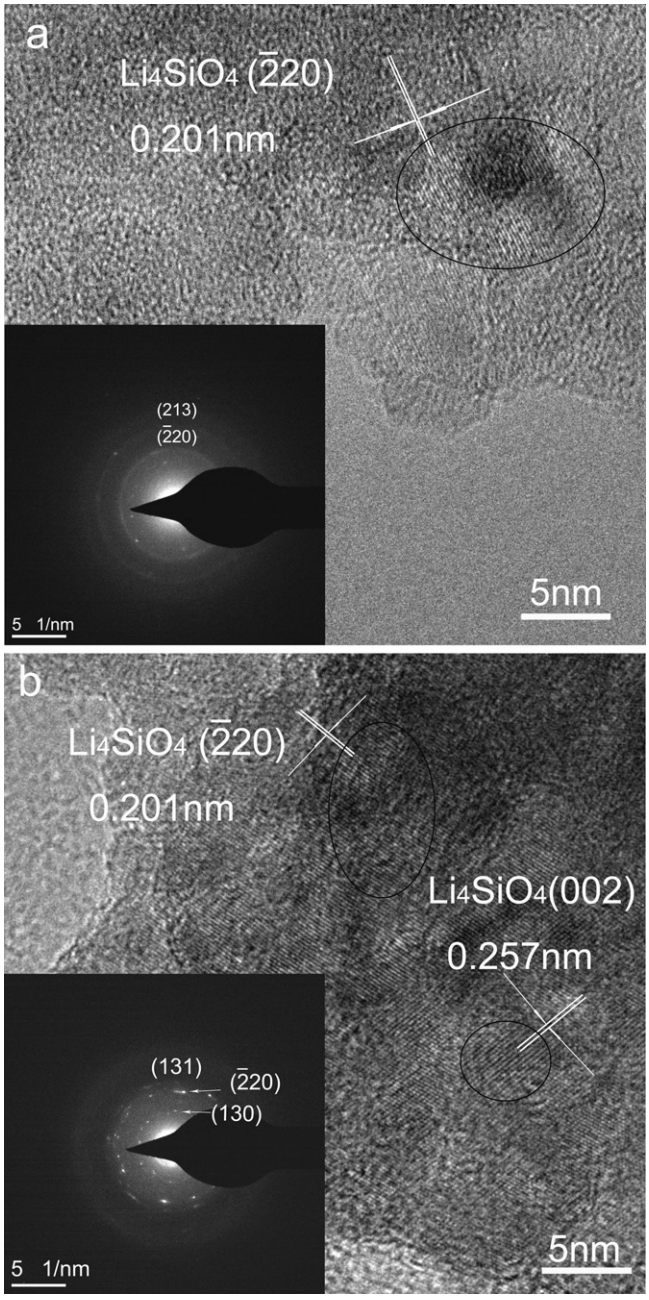

Fig. 5. HR-TEM images (inset: electron-beam diffraction patterns) of SiO_x/C electrodes discharged to 0.01 V (a) and charged to 3.0 V (b).

ture should be Li_4SiO_4. The lattice spaces of the ordered domains in Fig. (a) and (b) agree well with Li_4SiO_4 ($\bar{2}20$) plane spacing, and Li_4SiO_4 ($\bar{2}20$) and (002) plane spacing, respectively. Apparently, Li_4SiO_4 was irreversibly formed in SiO_x/C electrode during lithiation process, which is one of the origins of the large initial capacity loss. Li_4SiO_4, as irreversible product, was also found in other Si-based electrodes [18,19]. The lithiation reaction of SiO_x/C composite, therefore, might be suggested as follows:

$$2SiO_2 + 4Li^+ + 4e^- \rightarrow Li_4SiO_4 + Si \quad (1)$$

$$SiO_2 + 4Li^+ + 4e^- \rightarrow 2Li_2O + Si \quad (2)$$

$$Si + xLi^+ + xe^- \leftrightarrow Li_xSi \quad (3)$$

The SiO_2 domains in SiO_x particle is reduced to Si when the composite is initially discharged, as expressed in Eqs. (1) and (2), which is followed by the further lithiation of the reduced Si and the originally existing Si-cluster, as described in Eq. (3). Although no Li_2O is detected in the lithiated electrode, its existence cannot be completely excluded [18], it may take amorphous state. The irreversible formation of Li_2O and Li_4SiO_4 consumes much lithium, which should be responsible for the high irreversible capacity in the initial cycle.

4. Conclusions

Nano-sized SiO_x/C anode material with a core–shell structure is synthesized via the modified Stöber method. HR-TEM observation reveals that SiO_x with an O/Si ratio close to 1 is actually composed of amorphous Si clusters and well ordered SiO_2 domains. SiO_x/C anode material shows high reversible specific capacity (~800 mAh g^{-1}), excellent cycling stability and good rate-capability. Li_2O and Li_4SiO_4 are produced during the initial lithiation process, which consume great amount of lithium and thus cause large irreversible capacity loss. On the other hand, these oxides can act as buffer to prevent the agglomeration of derived Si-clusters and to accommodate the volume change caused by Si component and thus making big contribution to the cycleability of the electrode. The nano-scale characteristics of SiO_x/C particle ensures the fast Li-ion diffusion in the electrode and the carbon coating layer on the SiO_x particle surface renders the electrode having a good electronic conductivity. Both of them are accounted for the excellent rate-capability of SiO_x/C electrode.

Acknowledgments

This work was supported by Program for Guangdong Industry-Academy-Alliance Research (2009A090100020) and Program for New Century Excellent Talents in University of China (NCET-07-0072).

References

[1] A. Veluchamy, C. Doh, D. Kim, J. Power Sources 188 (2009) 574–577.
[2] J. Yin, M. Wada, K. Yamamoto, Y. Kitano, S. Tanase, T. Sakai, J. Electrochem. Soc. 153 (2006) A472–A477.
[3] M. Green, E. Fielder, B. Scrosati, M. Wachtler, J.S. Moreno, Electrochem. Solid-State Lett. 6 (2003) A75–A79.
[4] T.D. Hatchard, J.R. Dahn, J. Electrochem. Soc. 151 (2004) A838–A842.
[5] U. Kasavajjula, C. Wang, A.J. Appleby, J. Power Sources 163 (2007) 1003–1039.
[6] Y. Liu, Z.Y. Wen, X.Y. Wang, A. Hirano, N. Imanishi, Y. Takeda, J. Power Sources 189 (2009) 733–737.
[7] C. Doh, H. Shin, D. Kim, Y. Ha, B. Jin, H. Kim, S. Moon, A. Veluchamy, Electrochem. Commun. 10 (2008) 233–237.
[8] J. Kim, H. Sohn, H. Kim, G. Jeong, W. Choi, J. Power Sources 170 (2007) 456–459.
[9] X. Yang, Z. Wen, X. Xu, B. Lin, S. Huang, J. Power Sources 164 (2007) 880–884.
[10] W. StÕber, A. Fink, E. Bohn, J. Colloid Interface Sci. 26 (1968) 62–69.
[11] J. He, H. Zhao, J. Wang, J. Wang, J. Chen, J. Alloys Compd. 508 (2010) 629–635.
[12] T. Morita, N. Takami, J. Electrochem. Soc. 153 (2006) A425–A430.
[13] R.A. Nyquist, R.O. Kagel, Infrared Spectra of Inorganic Compounds (3800–45 cm^{-1}), Academic Press, Inc., New York, 1971.
[14] M. Mamiya, M. Kikuchi, H. Takei, J. Cryst. Growth 237–239 (2002) 1909–1914.
[15] S. Zhang, Z. Du, R. Lin, T. Jiang, G. Liu, X. Wu, D. Weng, Adv. Mater. 22 (2010) 5378–5382.
[16] L. Cui, R. Ruffo, C.K. Chan, H. Peng, Y. Cui, Nano Lett. 9 (2009) 491–495.
[17] Q. Sun, B. Zhang, Z. Fu, Appl. Surf. Sci. 254 (2008) 3774–3779.
[18] B. Guo, J. Shu, Z. Wang, H. Yang, L. Shi, Y. Liu, L. Chen, Electrochem. Commun. 10 (2008) 1876–1878.
[19] X. Yang, Z. Wen, L. Zhang, M. You, J. Alloys Compd. 464 (2008) 265–269.